

Article

# Utilisation of Water-Washing Pre-Treated Phosphogypsum for Cemented Paste Backfill

Yikai Liu <sup>1</sup>, Qinli Zhang <sup>1</sup>, Qiusong Chen <sup>1,\*</sup>, Chongchong Qi <sup>2</sup>, Zhu Su <sup>1</sup> and Zhaodong Huang <sup>1</sup>

<sup>1</sup> School of Resources and Safety Engineering, Central South University, Changsha 410083, China; yikai1995@foxmail.com (Y.L.); zhangqinlicn@126.com (Q.Z.); suzhu16@163.com (Z.S.); huangzhaodong1995@foxmail.com (Z.H.)

<sup>2</sup> School of Civil, Environmental and Mining Engineering, The University of Western Australia, Crawley 6009, Australia; chongchong.qi@gmail.com

\* Correspondence: qiusong.chen@csu.edu.cn; Tel.: +86-151-1627-9873

Received: 22 January 2019; Accepted: 9 March 2019; Published: 12 March 2019



**Abstract:** Recycling phosphogypsum (PG) for cemented paste backfill (CPB) has been widely used at phosphate mines in China. However, the impurities in PG prolong the setting time and reduce the uniaxial compressive strength (UCS), limiting the engineering application of PG. This paper aims to investigate the feasibility of treated PG (TPG) washed repeatedly using deionised water (DW) for CPB. A water-washing pre-experiment was first conducted to find the proportion with the least DW demand and the effects of water-washing on ordinary PG (OPG). Then, based on the PG:DW ratio obtained from the pre-experiment, the properties of the OPG-based CPB (OCPB) and TPG-based CPB (TCPB) were tested using slump tests, UCS tests, and microstructural analysis. The results show that (1) after 11 water-washings at the PG:DW ratio of 1:1.75, the pH of the supernatant (pH = 6.328) meets the requirements of Chinese standard GB 8978-1996. (2) Water-washing improves the particle gradation quality of PG and removes the soluble impurities adsorbed at the surface of PG crystals. (3) The initial slump values of TCPB are 0.19–1.15 cm higher than that of OCPB, furthermore, the diffusivity values of TCPB are better than the performance of OCPB, with 0.61–1.68 cm of superiority. (4) The UCS values of TCPB are up to 0.838 MPa, 1.953 MPa, and 2.531 MPa, after curing for 7, 14, and 28 days. These are 0.283 MPa, 0.823 MPa, and 0.881 MPa higher than that of OCPB, respectively. It can be concluded that water-washing pre-treatment greatly improves the workability and mechanical property of PG-based CPB. These results are of great value for creating a reliable and environmentally superior alternative for the recycling of PG and for safer mining production.

**Keywords:** phosphogypsum; purification; water washing; waste recycle; cemented paste backfill

## 1. Introduction

Phosphogypsum (PG) is the main solid waste from the production of ammonium phosphate and phosphoric acid raw materials. An industrial plant of phosphate fertilisers produces approximately 4–6 tonnes of PG for every ton of phosphoric acid produced. The total amount of PG produced up to 2006 was estimated to be around 6 billion tonnes. The annual production of PG worldwide was estimated to be around 160 million tonnes. The production of PG is increasing worldwide and could reach 200–250 million tonnes within the next decade or two [1]. Normally, PG is mostly composed of calcium sulphate dihydrate ( $\text{CaSO}_4 \cdot 2\text{H}_2\text{O}$ ) containing some impurities, such as phosphoric acid ( $\text{H}_3\text{PO}_4$ ), hydrofluoric acid (HF), heavy metals (Sr, Ba, Cu, Cd, etc.), and radioactive-elements ( $^{226}\text{Ra}$ ,  $^{238}\text{U}$ ) [1,2]. Historically, PG was disposed of on the Earth's surface, which not only wasted a lot of resources, but also caused serious pollution of the atmosphere, soil, and water near the burial locations [3–7].

The effective utilisation of PG as an industrial waste is closely related to the coordinated development of natural resources, environment, and economy. However, because of the physical and chemical characterisations of PG, strong acidity ( $\text{pH} < 3$ ) and high moisture content, only about 15% of PG has been reused in different fields such as soil stabilisation amendments, agricultural fertilisers, as set controller in cement manufacture, and in building materials [8–11]. Recently, researchers [12–14] have applied PG in cemented paste backfill (CPB) for use in underground mine stopes, which has been approved as an economic, safe, and environmentally friendly technology. Specifically, CPB is an engineered material created by the combination of different types of binders, tailings having different physical characteristics and the water [15–19]. In addition, owing to its high content of  $\text{CaSO}_4 \cdot 2\text{H}_2\text{O}$ , which produces insoluble  $\text{Ca}_3(\text{PO}_4)_2$  and hinders the hydration process, ordinary PG (OPG) is a typical cement retarder. Moreover, the impurities in OPG, such as HF and  $\text{H}_3\text{PO}_4$ , also prolong the setting time and reduce the uniaxial compressive strength (UCS) of CPB. In this case, researchers have suggested different methods to ensure the backfill quality of PG used as an alternative raw material for application in CPB [16–24]. These include, for instance, substantially increasing the proportion of ordinary Portland cement (OPC) in mixtures or adding other tailings, such as fly ash, waste lime and zeolite, as the hydration activators. Romero-Hermida et al. [25] investigated the rheological properties and microstructures of special lime putty prepared from PG. These methods decrease the setting time and improve the mechanical property of PG-based CPB. However, the cost is greatly increased, which substantially exceeds the resource capacity of (profitable) mining enterprises and limits the application of PG.

Therefore, many researchers tried to remove or at least reduce the impurities in PG to guarantee its safe use in the construction field. Taher [26] conducted a comparative study of PG with thermal treatments at different temperatures in an attempt to purify PG and improve its performance as a tailing. The results showed that thermal treatments can effectively improve the hydraulic properties of Portland slag cement and the best hydraulic properties of Portland slag cement occurred when using PG thermally treated at  $800\text{ }^\circ\text{C}$ . Singh [27] treated PG with aqueous citric acid solution, intending to convert phosphatic and fluoride impurities into water-removable citrates, aluminates and ferrates. The results of this study illustrated that the purified PG had less content of phosphates, fluorides and organic matter compared with the untreated material. Mun et al. [28] used 0.5% milk of lime at  $20\text{ }^\circ\text{C}$  to wash PG for 5 min (the ratio of PG:milk was 14%), after neutralisation treatment, the PG was dried at  $80\text{ }^\circ\text{C}$ . In this study, the pre-treated PG was not only considered as an effective activator, but also an impactful binder to granulated blast-furnace slag. Potgieter et al. [29] illustrated that treatment with ammonium hydroxide or sulphuric acid was effective in reducing set retardation of PG-based CPB. The above pre-treatment methods can remove the impurities in PG to different degrees, but the properties of the prepared mixture are different due to the different mechanisms of the pre-treatment methods. Meanwhile these methods are too complicated in the field for industrial practice. In this research, thus, a pre-treatment method, water-washing, was proposed to remove impurities from PG.

The pre-treatment of adding water and separating supernatant and precipitate by centrifuge is widely used as an effective and simple method of impurity removal in various industries. Kamimura et al. [30] studied an efficient purification method for washing recovered fibre-reinforced plastic monomer with water, which improved the hardness of recycled plastics and made them as hard as polyester made from virgin materials. Slavinskaya [31] used water to remove organic and mineral impurities at an industrial ion-exchange installation. Shuang et al. [32] investigated the possibility of using deionised water (DW) to remove chloride ions for inexpensive ultra-pure  $\text{TiCl}_4$ . Therefore, as a simple and mild pre-treatment method for purification, water-washing has potential application for PG-based CPB, especially considering that the  $\text{CaSO}_4 \cdot 2\text{H}_2\text{O}$  in PG is slightly soluble in water and most of the impurities, such as  $\text{H}_3\text{PO}_4$ , HF, and ammonium salt, are also soluble in water [33]. Cárdenas-Escudero et al. [34] demonstrated that the alkaline soda solution can effectively dissolve PG and form the portlandite precipitation.

In the present study, investigations were carried out to study the chemical and physical optimisations of water-washing pre-treatment to PG for using as the raw materials in PG-based CPB. A water-washing pre-experiment was firstly conducted to optimise the proportion of PG:DW recording the total nitrogen (TN), chloride ion concentration (Cl), fluoride concentration (F), total phosphorus (TP), conductance (Cond) and pH parameters of the supernatant liquid in each washing. Then, scanning electron microscopy (SEM), X-ray diffraction (XRD) analysis, X-ray fluorescence (XRF) analysis, and particle size tests were conducted. Secondly, the properties of OPG-based CPB (OCPB) and treated PG (TPG)-based CPB (TCPB) were determined using slump tests, diffusivity tests, UCS tests, and microstructural analysis. The flow chart of this work is shown in Figure 1.

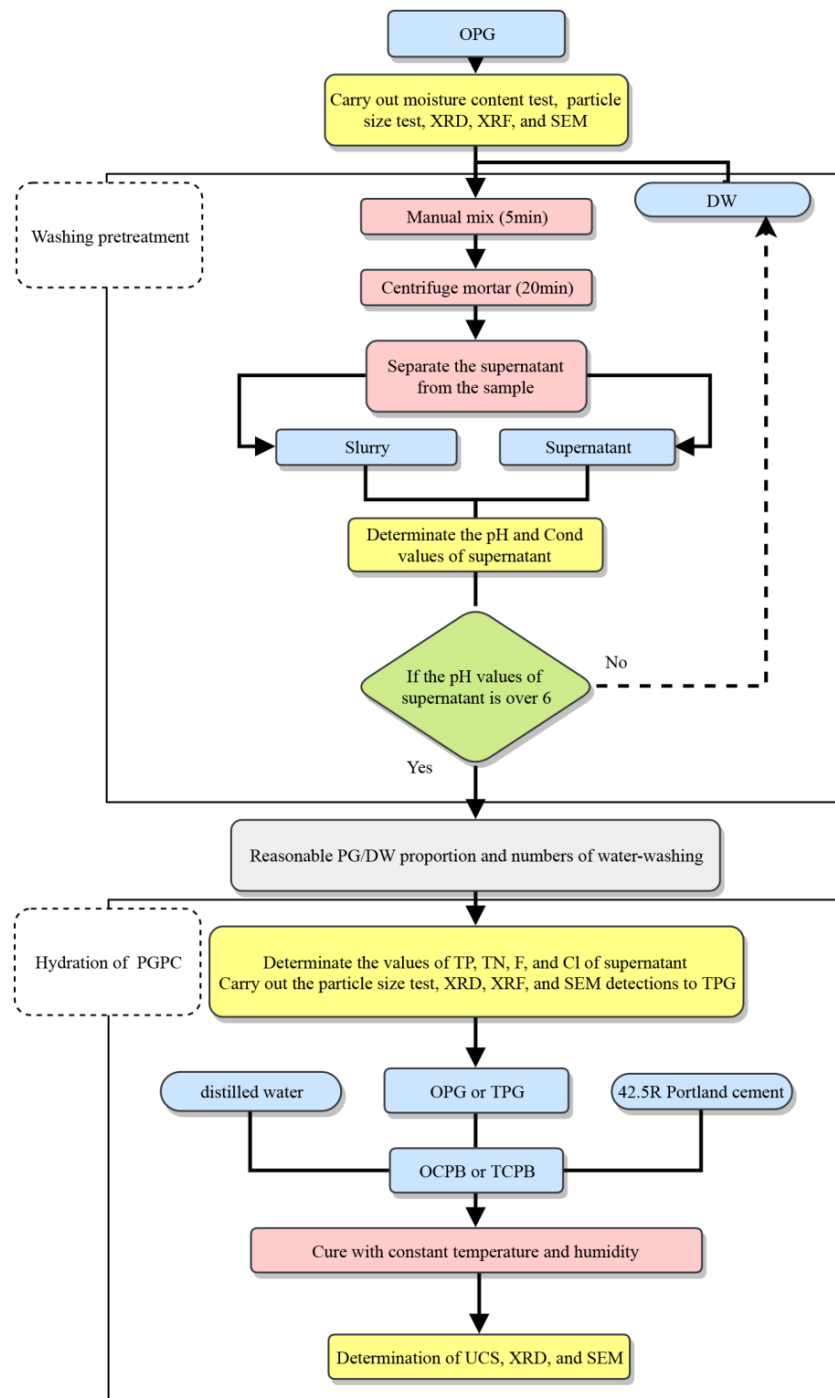


Figure 1. Flow chart of the experiments.

## 2. Materials and Methods

### 2.1. Raw Materials and Water-Washing Pre-Treatment

OPC 42.5R (similar to ASTM C150 Type I cement [35]) and OPG with moisture content of 18.26%, natural density (wet) of 1.62 g/cm<sup>3</sup>, and dry density of 0.86 g/cm<sup>3</sup> (heated for 24 h, 95 ± 5 °C), which was obtained from a phosphoric acid factory named Western Chemical Co. Ltd., plant (Yichang, China), were used in this work. The physical properties and chemical compositions of OPC and OPG are shown in Tables 1 and 2, respectively, and the particle size distribution of OPG and OPC are shown in Figure 2, the data were provided using a laser particle size tester (Master Sizer 2000, Malvern Instruments Ltd., Malvern, UK). As stated above, the main components of OPG are SO<sub>3</sub> (41.504%) and CaO (44.897%), with a small amount of P<sub>2</sub>O<sub>5</sub> (1.224%) and F (0.817%). The particle size of OPG ranges from 0.710 μm to 255.53 μm and the mean particle size ( $D_{50}$ ) is 58.329 μm. In addition, the water used in the washing pre-treatment was DW (produced by Solar-bio Co. Ltd., Beijing, China) to avoid the effects of ions, while the water used in the hydration of OCPB and TCPB was ordinary distilled water.

**Table 1.** Chemical compositions of ordinary Portland cement (OPC) and ordinary phosphogypsum (OPG).

Chemical Composition (%)	OPC	OPG
Na <sub>2</sub> O	0.090	0.150
MgO	1.840	0.111
Al <sub>2</sub> O <sub>3</sub>	4.420	0.782
SiO <sub>2</sub>	17.94	5.730
P <sub>2</sub> O <sub>5</sub>	0.215	1.224
SO <sub>3</sub>	3.400	41.504
Cl	0.022	-
K <sub>2</sub> O	0.671	0.674
CaO	60.850	44.897
TiO <sub>2</sub>	0.307	0.648
V <sub>2</sub> O <sub>5</sub>	0.040	-
Cr <sub>2</sub> O <sub>3</sub>	0.025	-
MnO	0.265	-
Fe <sub>2</sub> O <sub>3</sub>	3.814	3.208
CuO	0.015	-
ZnO	0.043	-
Rb <sub>2</sub> O	0.003	-
SrO	0.067	0.142
ZrO <sub>2</sub>	0.010	-
BaO	0.034	0.113
F	-	0.817
Loss	5.929	-

**Table 2.** Physical properties of OPC and OPG.

Physical Properties	OPC	OPG
SSA (m <sup>2</sup> /g)	1.690	0.324
$D_{[4,3]}$ (μm)	24.449	69.935
$D_{10}$ (μm)	1.426	13.176
$D_{50}$ (μm)	14.641	58.329
$D_{90}$ (μm)	64.392	146.589
$D_{d<20 \mu m}$ (%)	57.84	81.78
Moisture content (%)	-	18.26
Natural density (g/cm <sup>3</sup> )	2.94	1.62
Dry density (g/cm <sup>3</sup> )	-	0.86

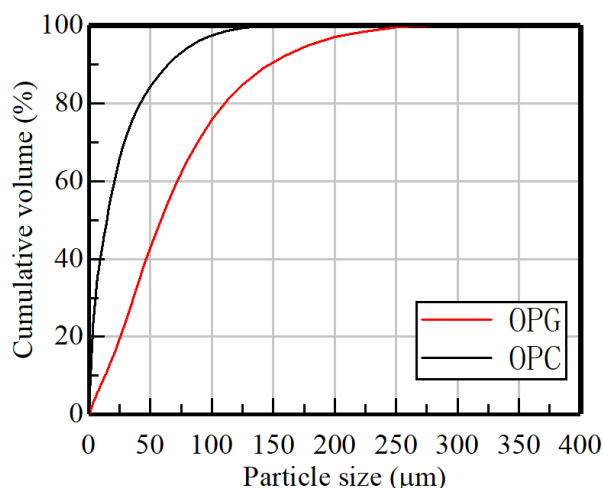


Figure 2. Particle size distribution of OPG and OPC.

In this study, eight PG:DW ratios were used in the pretreatment, ranging from 0.4 to 2.0. The PG measure was wet weighed before mixing with DW of certain qualities according to Table 3 and then artificially stirred for 5 min in a steel blender (TD5M low-speed desktop centrifuge, produced by Shanghai Lu Xiangyi Centrifuge Instrument Co. Ltd., Shanghai, China), subsequently, the uniformly mixed materials were centrifuged for 20 min at 300 r/min. According to the Chinese standard of surface water environmental quality [36], the fifth-class surface water (suitable for agricultural water and water for general landscapes, etc.) is guaranteed because the content of TP, TN, F are less than 0.4, 2.0, 1.5 mg/L. Besides, in central drinking water surface, the content of Cl in the discharged water should be less than 250 mg/L. Therefore, after centrifugation, the supernatant was taken out to determine the pH and Cond using a multiparameter analyser (produced by INESA, DZS-708L multiparameter controller), ionic electrodes (produced by INESA, BestLab water pH composite electrode), and a conductance electrode (produced by INESA, DJS-10C conductance electrode). The washing process was repeated until the pH of supernatant fully met the requirements of Chinese standard (pH > 6) [37]. The measured supernatant was collected in plastic sealed cups and kept at  $25 \pm 2$  °C using a thermostat. The content of F and Cl were tested using the same multiparameter analyser and other ionic electrodes produced by INESA (PF-202-C fluorine ion composite electrode, PCL-1-01 chloride ion electrode). The values of TP and TN were determined using a water quality measurement instrument (5B-6C-V8, produced by Lianhua Science and Technology Co. Ltd., Beijing, China). The electrodes were washed with DW after each measurement.

Table 3. Mix proportions of OPG samples.

No.	Weight of OPG		DW (g)	PG:DW	Number of Washes	Total DW (g)
	Wet (g)	Dry (g)				
A	1000.00	817.40	226.10	1:0.50	79	17,861.90
B	1000.00	817.40	430.45	1:0.75	46	19,800.70
C	1000.00	817.40	634.80	1:1.00	37	23,487.60
D	1000.00	817.40	839.15	1:1.25	28	23,496.20
E	1000.00	817.40	1043.50	1:1.50	19	19,826.50
F	1000.00	817.40	1247.85	1:1.75	11	13,726.35
G	1000.00	817.40	1452.20	1:2.00	10	14,522.00
H	1000.00	817.40	1860.90	1:2.50	8	14,887.20

## 2.2. Mix Proportions and Cemented Paste Backfill (CPB) Preparation Process

As shown in Table 4, there were 12 different mix-proportions of PG-based CPB with all materials being calculated by mass percent. In accordance with the above proportions, all solid materials were

weighed and mixed in the planetary mixer for 30 s before adding water. In addition, when weighing the raw materials, PG was considered as dry mass by subtracting the water content. After that, raw materials were stirred homogeneously for 5 min and the premixed mixture was casted into plastic cylindrical moulds [38] (diameter of 5 cm and height of 10 cm). After 24 h of hydration, specimens were taken out of the moulds and moved into a standard chamber with constant temperature and humidity ( $25 \pm 2$  °C and  $90 \pm 5\%$ , respectively).

**Table 4.** Mix proportions of PG-based cemented paste backfill (CPB).

No.	OPC	OPG (Dry)	TPG (Dry)	Water	Water/Solid	Water/Cement
1-OPG	8.57%	62.92%	-	28.51%	0.67	3.33
2-OPG	8.86%	65.01%	-	26.13%	0.61	2.95
3-OPG	6.67%	65.25%	-	28.09%	0.67	4.21
4-OPG	6.89%	67.42%	-	25.69%	0.61	3.73
5-OPG	5.45%	66.73%	-	27.82%	0.67	5.10
6-OPG	5.64%	68.95%	-	25.41%	0.61	4.51
1-TPG	8.57%	-	62.92%	28.51%	0.67	3.33
2-TPG	8.86%	-	65.01%	26.13%	0.61	2.95
3-TPG	6.67%	-	65.25%	28.09%	0.67	4.21
4-TPG	6.89%	-	67.42%	25.69%	0.61	3.73
5-TPG	5.45%	-	66.73%	27.82%	0.67	5.10
6-TPG	5.64%	-	68.95%	25.41%	0.61	4.51

### 2.3. Test Methods

#### 2.3.1. Test of X-ray Fluorescence (XRF)

Elemental analysis was carried out on a Bruker S4 Pioneer XRF analyser (Bruker, Billerica, MA, USA) and the samples were processed by the conventional pressing plate method. The samples were first ground into powder by a grinder, after which they were heated in an oven at  $45 \pm 5$  °C for 24 h. Then, 2 g of the processed sample was accurately weighed and blended well with 2 g of boric acid in an agate mixture. Next, the mixed powder was loaded into a die and compacted (60 s at 40 t pressure) into a circular plate with a diameter of 32 mm and an outer diameter of 40 mm using the boric acid to pad the bottom edge. Samples were labelled and preserved in a dry and pollution-free environment after pressing and then analysed using full quantitative analysis without standard samples.

#### 2.3.2. Test of Abrams Cone

Much of the research was to determine if the CPB mixture with a slump value over 170 mm could be successfully transported underground by backfill pumps [39–41]. Therefore, in this study, trial slump tests [9] were conducted to make sure that the slump values of the OCPB and TCPB mixtures were greater than 170 mm. The preparation of materials and the test process were in accordance with the standard test method for slump [42]. The premixed mixture was casted into a conical mould (the top diameter of 10 cm, the bottom diameter of 20 cm and height of 30 cm) with a plate glass at the bottom. After that, the conical mould was lifted about 10 cm and the previously constrained mixture slurry flowed down freely. The values were measured diagonally and vertically when the mixture stopped flowing and the result was determined by the average of two repeated experiments.

#### 2.3.3. Test of Uniaxial Compressive Strength (UCS)

As a widely used detection mean of the mechanical properties of CPB for exploring an efficient mix design and reaching a higher performance in underground mining structures [43], the standard UCS tests were carried out in this study. For each ratio, there were three corresponding specimens. The UCS tests were carried out according to the ASTM Standard C39 C39M-2014a [44]. After curing for 7, 14, or 28 days, the specimens were subjected to unconfined compressive strength tests using an

anti-bending machine (23 MTS Insight, MTS Systems Co. Ltd., Eden Prairie, MN, USA) with 30 kN loading capability at a displacement rate of 0.1 mm/min. Each test was performed in triplicate and the mean value was used for further analysis.

#### 2.3.4. Microstructural Analysis

After the UCS tests, samples were taken from the broken surfaces and then immersed in plastic bottles of acetone solvent in order to terminate the hydration, which bottles were then sealed. Then, superfluous solution was removed using a vacuum filter after 24 h of immersion. The treated samples were studied using a JSM-6490LV scanning electron microscope (JEOL Ltd., Beijing, China). XRD analysis of the samples was performed using an X-ray diffractometer (D8 Advance, Bruker, Karlsruhe, Germany) with  $\text{CuK}\alpha$  radiation and Ni filter. The XRD patterns were appraised using the references in the PDF-2 data base (PDF-2 International Centre for Diffraction Data, Newtown Square, PA, USA).

### 3. Results and Discussion

#### 3.1. Effect of Washing Pre-Treatment on Phosphogypsum (PG)

##### 3.1.1. Changes of pH, Conductivity and Values of the Ions in the Supernatant

Table 3 shows the number of water-washing pre-treatments required for different PG:DW proportions. With increase of the PG:DW ratio, the number of washings required increases from 8 to 79. However, the amount of DW required increases to a peak at the PG:DW ratio of 1:1.25 (23,496.20 g); then drops to a bottom at the ratio of 1:1.75 (13,726.35 g). Finally it rises back to 14,887.20 g at the smallest ratio of 1:2.50. Moreover, as is shown in Figure 3a, the Cond values of the different proportions are stable at about 2.00 with increase in the number of washings. After several times of centrifugation, the ions dissolved in water are separated from the PG mixture into the supernatant. This means that stable conductivity is regarded as a sign of the successful washout of soluble impurities in the PG. As regards the changes in pH of the supernatant, Figure 3b shows the variation curves for the different proportions and shows that all the values increase greatly in the first several washings; then the pace of change gradually slows down. This means that in the early stage of the washing process, large quantities of soluble acidic substances in the PG are dissolved in the liquid phase and the conclusion is also consistent with the conductivity of the supernatant. Therefore, taking the amount of DW into consideration, the PG was washed 11 times using DW with PG:DW value of 1:1.75, for use in subsequent experiments.

Figure 4 shows the changes in the dissolved ion concentration in the supernatant with the number of water-washing pre-treatments. At the PG:DW value of 1:1.75, the principal axis demonstrates the content of TN, F and Cl, and the ordinate axis shows the content of TP. After being washed and centrifuged once, the contents of TP, TN and Cl in the supernatant were 5943.78, 23.23 and 264.33 mg/L, respectively. With an increase in the number of washings, the values of TP, TN, and Cl decrease continuously to 10.33, 0.19, and 10.45 mg/L. In contrast, for the first three times, the value of F increases from 30.22 to 52.30 mg/L; then gradually decreases to 12.19 mg/L. The possible reason for the obvious increase in F content is that soluble F mainly occurs in the form of sodium fluoride (NaF) compounds in PG. Meanwhile, as a weak acid, the hydrogen and F ions in the solution form HF only in the highly acidic liquid phase. Therefore, during the initial washing processes, it was easy for the F compounds, which are sparingly soluble in water, to combine with H ions to form HF in the strong acidic liquid phase, thereby causing an increase in the concentration of F in the supernatant. With increase in pH values, the fluoride ions dissolved in the liquid phase were discharged with the supernatant, thus the F-content decreases gradually. Although the content of TN, TP, F, and Cl has eventually decreased after repeated water-washing pre-treatment, the figures are still higher than the

standard for direct emission, so the polluted water needs to be put into the sewage treatment plant for further purify as the recycled-water for the concentrator [45].

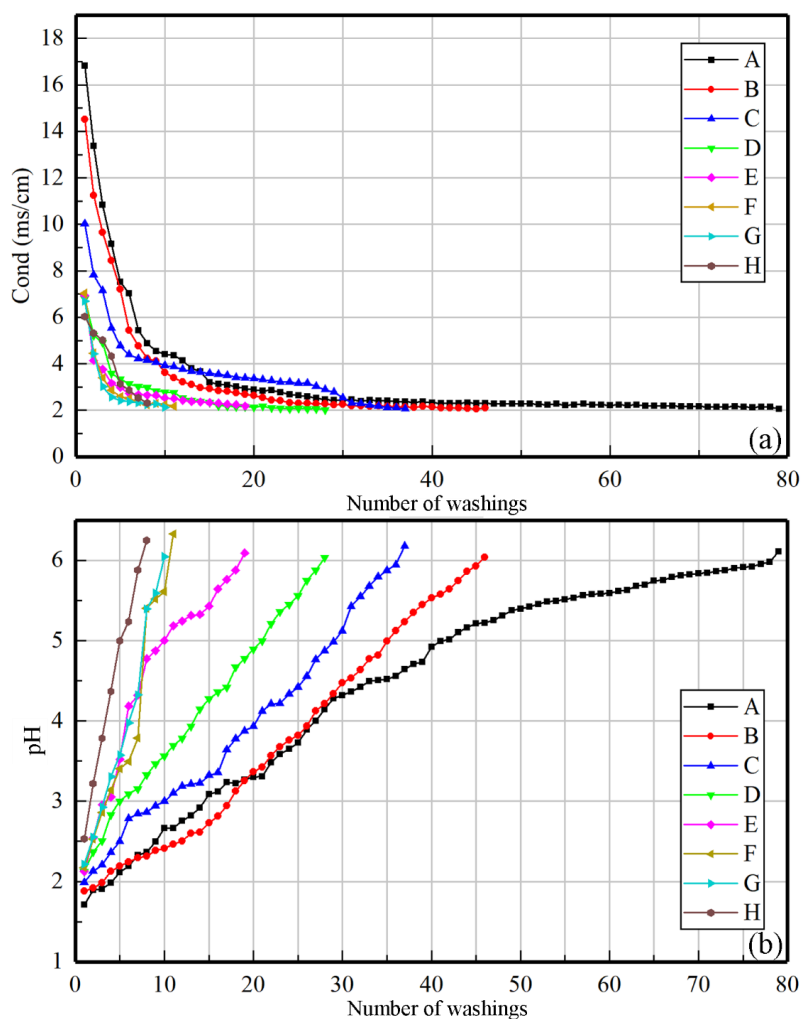


Figure 3. Cond (a) and pH (b) values of the supernatant.

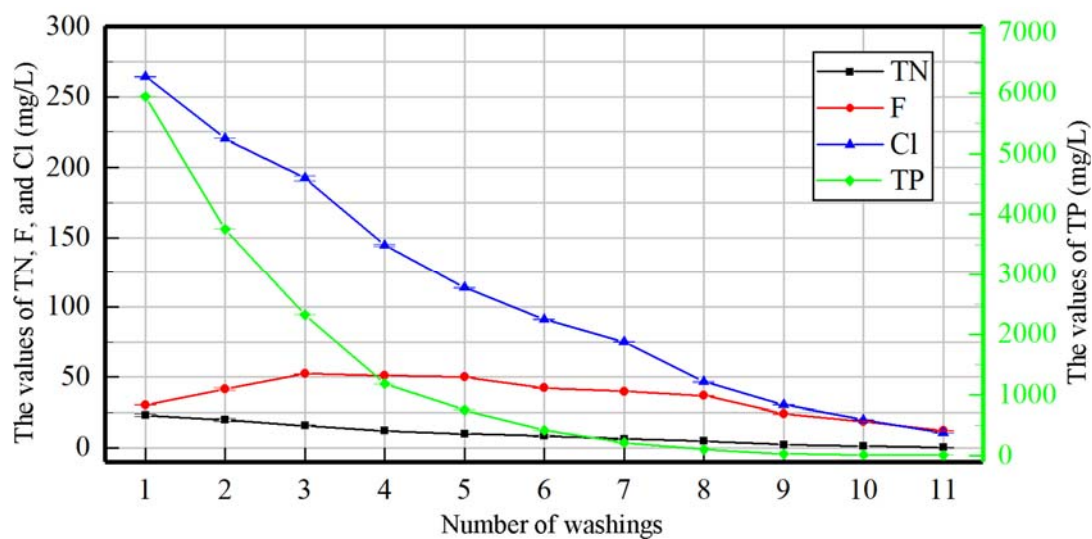


Figure 4. Values of the ion concentration in the supernatant.

### 3.1.2. Analysis of XRF

As shown in Tables 1 and 5, CaO, SO<sub>3</sub>, and SiO<sub>2</sub> are both the main components of OPG and TPG. After the water-washing pre-treatment, the content of CaO and SO<sub>3</sub> in TPG are slightly increased, while the other chemical components decreased relatively. Among them, the content of Fe<sub>2</sub>O<sub>3</sub> exhibited the greatest reduction, from 3.208% to 0.663%, which indicates the partial loss of Fe during filtration of the supernatants. Moreover, the content of the impurity P<sub>2</sub>O<sub>5</sub> obviously also decreased, from 1.224% to 0.714%. In addition, the impurity MgO was hardly detected in TPG (0.005%), for which the possible reason is that all the MgO exists in PG in the form of water-soluble Mg compounds. The content of the impurities SiO and F in PG showed a modest decrease, while the content of other impurity elements in PG, such as Sr, Ti, and Ba, changed little, suggesting that these were insoluble in water. Therefore, the water-washing pre-treatment can effectively remove some of the soluble compounds in PG, whereas other impurities that are insoluble will likely be difficult to remove.

**Table 5.** Chemical compositions of TPG.

Chemical Composition (%)	Na <sub>2</sub> O	MgO	Al <sub>2</sub> O <sub>3</sub>	SiO <sub>2</sub>	P <sub>2</sub> O <sub>5</sub>	SO <sub>3</sub>	K <sub>2</sub> O
TPG	0.065	0.005	0.300	5.194	0.714	45.014	0.298
Chemical Composition (%)	CaO	TiO <sub>2</sub>	Fe <sub>2</sub> O <sub>3</sub>	SrO	BaO	F	Loss
TPG	46.526	0.526	0.663	0.067	0.096	0.532	-

### 3.1.3. Analysis of Scanning Electron Microscopy (SEM)

Microstructures of OPG and TPG are shown in Figure 5. The crystal grains of OPG and TPG are both rhombic plate particles, which indicates that washing does not change the grain shape of PG. Figure 5a shows that the grain size distribution of OPG was irregular with a lot of small crystals adsorbed on the surface of PG crystal resulting in rough areas of the crystal surface. From Figure 5b, it can be seen that TPG has better surface smoothness with only a small part flocculent crystal but most were columnar and rhombic plates. Apparently, the crystalline form of TPG is better than OPG, with a more complete grain. Besides, although the materials have been washed several times, the particle morphology of TPG is mostly maintained, with a majority of water-soluble impurities removed from the surface of PG.

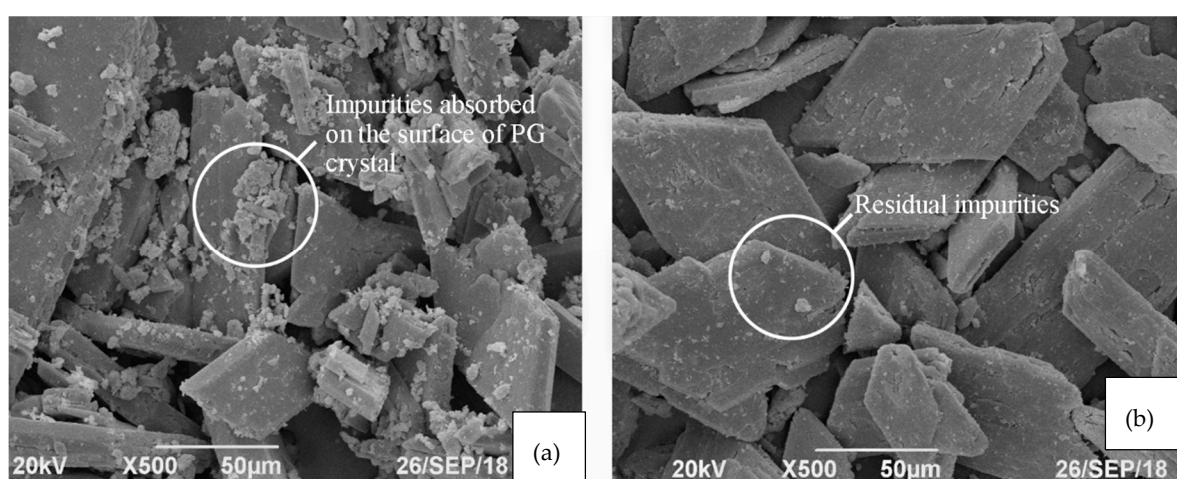


**Figure 5.** Scanning electron microscope (SEM) images of the OPG (a) and the TPG (b).

### 3.1.4. Analysis of the Particle Size

Table 2, Table 6, and Figure 6 illustrate the particle size of OPG and TPG. The particle size of TPG is obviously smaller, and ranges from 0.0796 µm to 251.785 µm. It is clear that the specific surface

area (SSA) and mean-volume diameter ( $D_{[4,3]}$ ) of PG decreased from 0.324 to 0.277 m<sup>2</sup>/g and from 69.935  $\mu\text{m}$  to 66.801  $\mu\text{m}$ , respectively, after water-washing pre-treatment. The particle size fitting formulas of OPG and TPG are shown in Equations (1) and (2).

$$C = (1.54224013 \times 10^{-6})x^3 + (-2.97030817 \times 10^{-3})x^2 + 1.03958678x - 0.24821556 \quad (R^2 = 0.99881838) \quad (1)$$

$$C = (2.63095018 \times 10^{-6})x^3 + (-3.12349930 \times 10^{-3})x^2 + 1.0208419x - 0.80246342 \quad (R^2 = 0.99776654) \quad (2)$$

**Table 6.** Particle size characters of TPG.

Physical Properties	SSA (m <sup>2</sup> /g)	$D_{[4,3]}$ ( $\mu\text{m}$ )	$D_{10}$ ( $\mu\text{m}$ )	$D_{50}$ ( $\mu\text{m}$ )	$D_{90}$ ( $\mu\text{m}$ )	$D_{d<20 \mu\text{m}}$ (%)
TPG	0.277	66.801	9.265	57.593	133.816	84.91

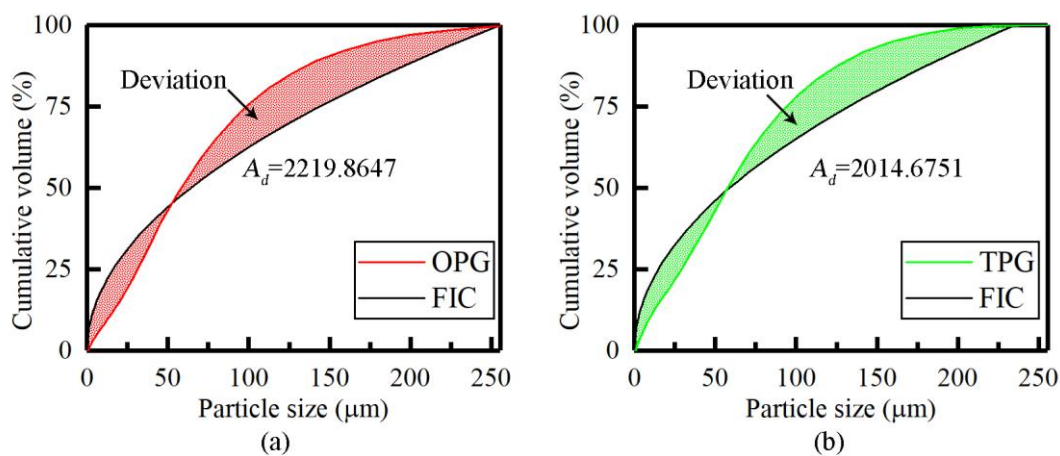


**Figure 6.** Particle size curve and Fuller ideal curve (FIC) of OPG (a) and TPG (b).

According to the maximum density curve theory proposed by W.B. Fuller et al. [46,47] and Yao [48], it is considered that the closer the tailings gradation curve is to a parabola, the smaller the void between particles and the maximum density. This is mainly used to describe a particle size distribution with continuous gradation. The equation of the Fuller ideal curve (FIC) gradation theory is as follows:

$$P_i = 100 \left( \frac{x_i}{D_{\max}} \right)^{0.5} \quad (3)$$

where  $x_i$  is the particle size of grade  $i$  tailings (mm),  $D_{\max}$  is the maximum particle size of tailings (mm) and  $P_i$  is the passing rate of  $x_i$  particles (%). In order to analyse qualitatively the particle size differences of TPG and OPG, the results were calculated using Equation (4) and the curves are shown in Figure 6a,b. The gradation curves of OPG and TPG both obviously deviate from the FIC. Therefore, to study further the influence of water-washing pre-treatment on the gradation of OPG, the area of the tailing's gradation curve deviating from the FIC was used to express the effect; the bigger the deviation area is, the worse the gradation of the raw material is. The area values were calculated using the following equation:

$$A_d = 100 \int_a^b [f(x) - P_i(x)] dx \quad (4)$$

where  $A_d$  is the area of tailings gradation curve deviating from ideal Fuller curve,  $a$  is the smallest particle size of the raw material and  $b$  is the largest particle size of the raw material. The values of  $A_d$  are shown in Figure 6, which illustrates that water washing can effectively optimise the particle size gradation with a difference value of 205.1896. Thus, the particle size distribution of PG can be obviously optimised by water-washing pre-treatment, which is closely related to the improvement of UCS values.

### 3.1.5. Analysis of X-ray Diffraction (XRD)

The results from investigating the purification of PG by washing repeatedly with DW are shown in Figure 7 (XRD patterns of the OPG and the TPG). The mineral phases of the TPG determined from the XRD patterns were  $\text{CaSO}_4 \cdot 2\text{H}_2\text{O}$ ,  $\text{CaSO}_4 \cdot 0.5\text{H}_2\text{O}$ ,  $\text{CaSO}_4$ , and  $\text{SiO}_2$ . In the case of OPG,  $\text{CaSO}_4 \cdot 0.5\text{H}_2\text{O}$ , and  $\text{CaSO}_4$  were undetected. Obviously, the main mineral phases in the OPG and TPG were both  $\text{CaSO}_4 \cdot 2\text{H}_2\text{O}$  and  $\text{SiO}_2$ . However, after being treated,  $\text{CaSO}_4 \cdot 2\text{H}_2\text{O}$  in OPG changed to  $\text{CaSO}_4 \cdot 0.5\text{H}_2\text{O}$  and  $\text{CaSO}_4$ , resulting in a decline in the content of  $\text{CaSO}_4 \cdot 2\text{H}_2\text{O}$  from 98.36% to 83.65%. The reaction equations [49,50], which generally go through the process of dissolution and recrystallisation, are as follows. The equilibrium of Equation (5) is susceptible to the influence of ions in liquid phase and to temperature, which trends to the right side with increasing concentration of  $\text{H}_3\text{PO}_4$ ,  $\text{H}_2\text{SO}_4$ , and temperature. Therefore, the presence of phosphate compounds in PG, which form  $\text{H}_3\text{PO}_4$  in the liquid phase, is one possible factor for the appearance of  $\text{CaSO}_4 \cdot 0.5\text{H}_2\text{O}$  in the TPG. However, the crystals of  $\text{CaSO}_4 \cdot 0.5\text{H}_2\text{O}$  are metastable and direct dehydration of  $\text{CaSO}_4 \cdot 2\text{H}_2\text{O}$  can form  $\text{CaSO}_4$ .

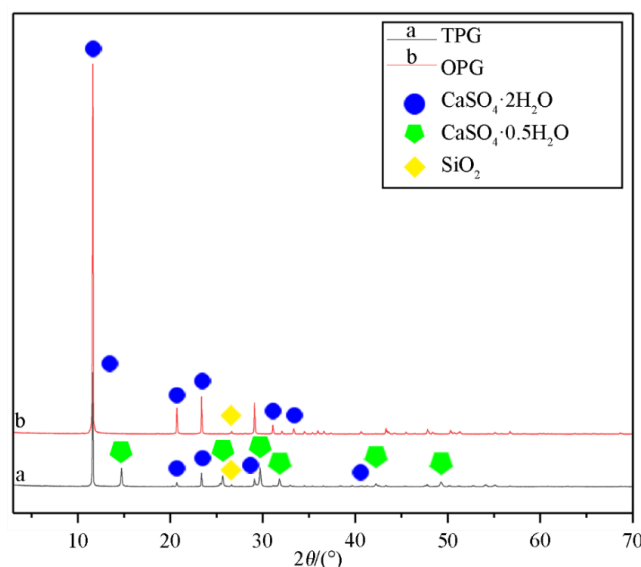
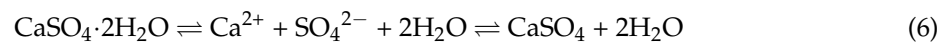
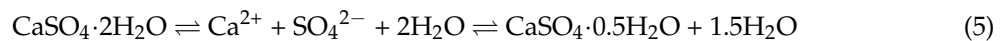
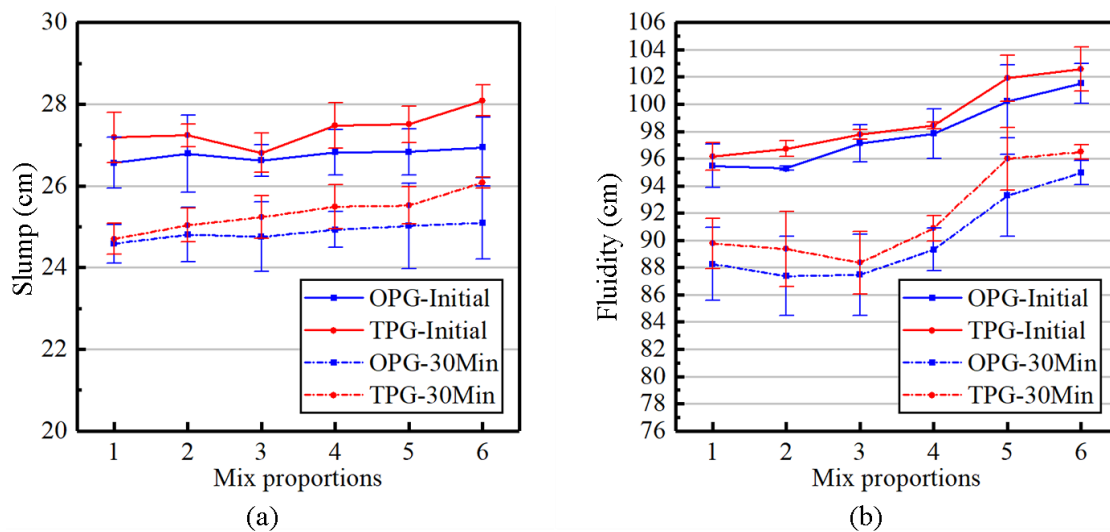


Figure 7. X-ray diffraction (XRD) patterns of OPG and TPG.

### 3.2. The Workability of PG-Based CPB

In order to analyse the effect of water-washing pre-treatment on the initial and 30 min aging workability of PG-based CPB to obtain relatively qualified workability values, slump and diffusivity tests were carried out. The results of the workability tests of OCPB and TCPB are demonstrated in Figure 8a,b, respectively. The results show that water-washing pre-treatment can obviously optimise the workability of TCPB mixture, furthermore, the slump and diffusivity performances for 30 min of TCPB mixture are still better than that of OCPB regardless of the content of PG, although the rules for increasing the slump and fluidity of the mixtures with different concentrations vary slightly. With an increase of the PG content, the effect from optimisation is more obvious and is at maximum at mix-proportion 6, where the figure for TCPB is 104.5% of OCPB. Meanwhile, the trend is more evident in the mixtures after aging for 30 min, despite the fact that the ratio remains at 104.0%. As regards

the values for fluidity of tailings, the initial TCPB mixtures have greater liquidity, compared with the OCPB mixtures, especially at mix-proportion 5, the fluidity of initial and 30m in hydration TCPB tailings are both 102.5% of OCPB.



**Figure 8.** Workability of the mixtures with OPG and TPG. (a) Values of slump; (b) values of fluidity.

### 3.3. The UCS of PG-Based CPB

Compressive strength is one of the most important factors used to measure the quality of backfill. According to the previous publications, the required static strength of CPB curing for 28 days without exposures is arbitrarily selected at 0.2 MPa [51,52]. Besides, much of the research [24] on backfill tailings have determined that mixtures with PG have little strength in 7 days, but that the strength increases rapidly in the middle and later stages. In addition, studies [7,14] of receiver biases suggest that the required strength of PG-based CPB is about 1 MPa at 28 days curing time. Figure 9 summarises the evolution of the UCS values for the OCPB and TCPB samples which all increase with curing age, despite that the growth rate varies with different stages. The 7 days UCS of OCPB is only 0.140–0.555 MPa, however, the value of UCS increases significantly with increase of the mass concentration and cement content: eventually it reaches 0.499–1.111 MPa. Although the general rule for UCS growth is also applied to the evolution of TCPB, the UCS of TCPB is much greater than that of OCPB under the same mix proportion. The 7 days UCS of TCPB is from 0.482 MPa to 0.838 MPa. At 14 days, the strength values are from 0.710 MPa to 1.100 MPa and the values at 28 days climbed to the maximum range 0.825–2.531 MPa.

The ratios of 7, 14, and 28 days UCS values of OCPB/TCPB is shown in Figure 10. It can be seen that the ratio of 7 days UCS ranges from 28.9% to 67.3%, then the ratio gradually stabilises at nearly 65.5% with increase of the curing age. Furthermore, the ratio of mix-proportion four remains near 70%. One of the possible factors associated with this phenomenon is the cementitious activity of PG, which can replace OPC under certain conditions of alkaline activation. One of the possible factors [53] associated with the stronger retarding phenomena of the OCPB is the soluble phosphate in the OPG that reacted with  $\text{Ca}^{2+}$  ions and formed a thin film covering the cement clinker particles, which slowed down the early hydration process of the OPC. However, the film is broken with the hydration proceeds, and the later strength development will not be deteriorated. Therefore, according to the XRF results, soluble phosphorus in OPG separated from PG crystal with water-washing, as a result, this deterioration of mechanical properties of PG-based CPB was weakened. However, with the hydration reaction, the film in PG-based CPB is broken, and the 14 and 28 days UCS values of OCPB increase rapidly.

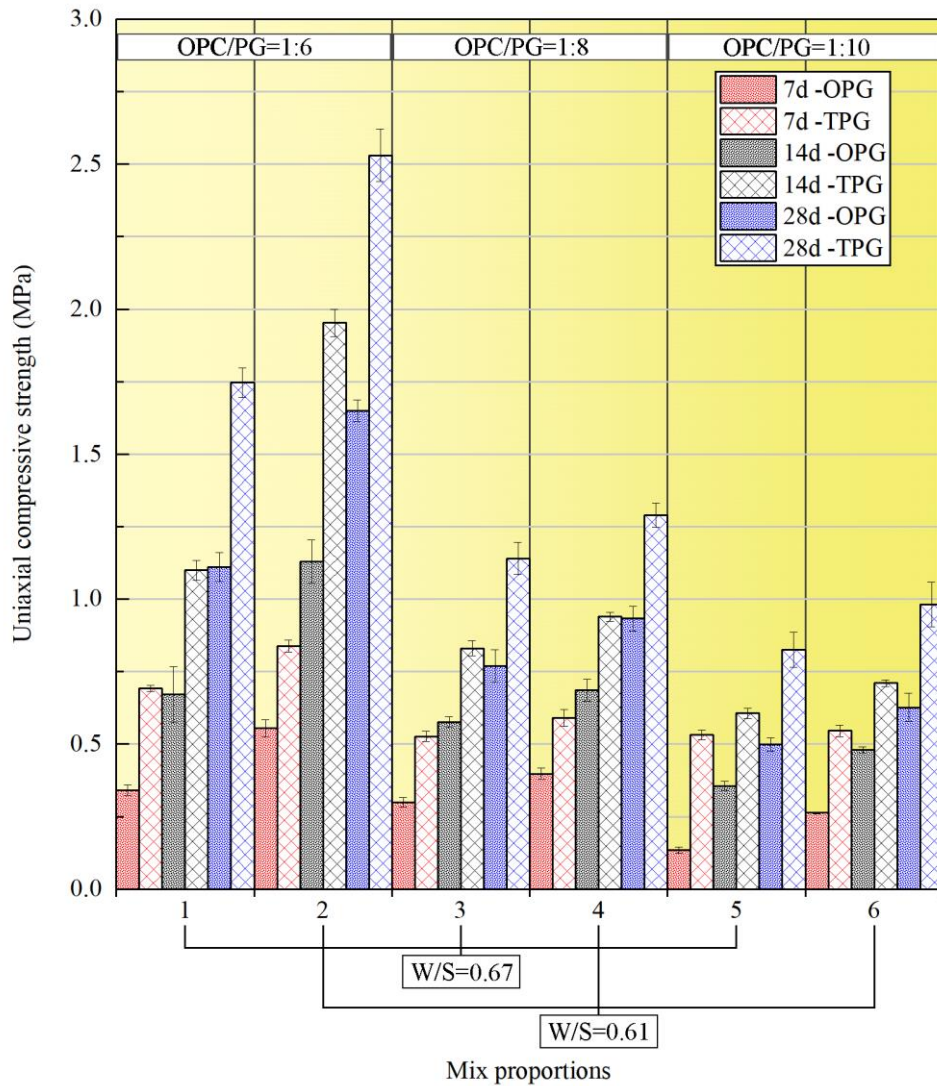


Figure 9. Uniaxial compressive strength (UCS) comparison of OPG-based CPB (OPCB) and treated PG (TPG)-based CPB (TCPB).

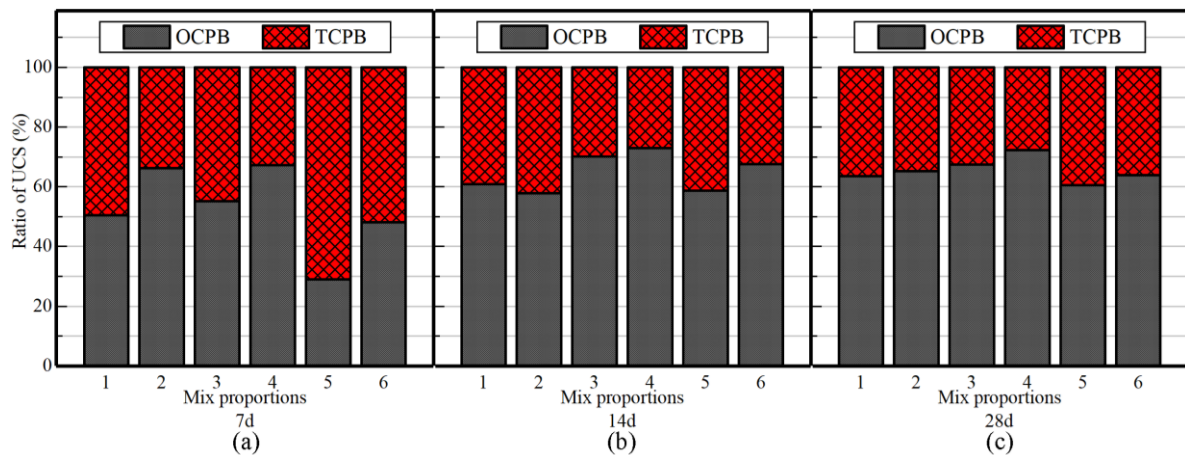
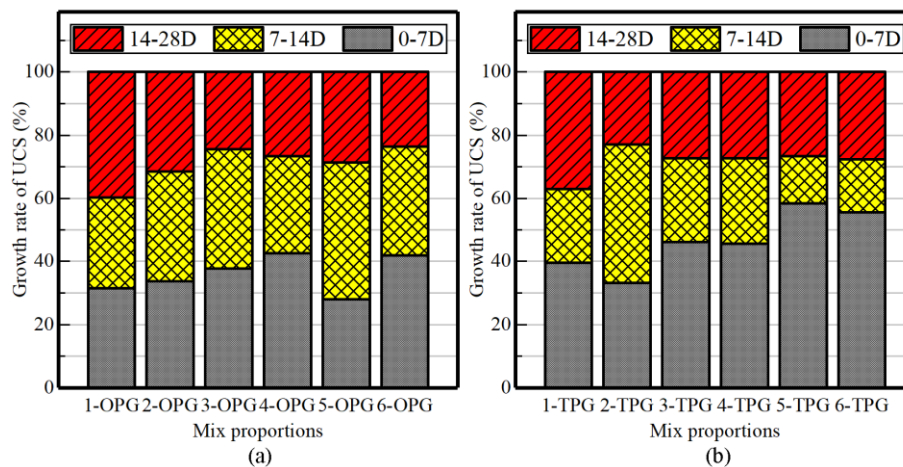


Figure 10. Growth rate ratio of OCPB and TCPB at (a) 7 days, (b) 14 days, and (c) 28 days.

In order to investigate the influence of OPG and TPG on strength growth of PG-based CPB in different curing ages, the strength growth rates of OCPB and TCPB at 0–7 days, 7–14 days and 14–28 days were calculated, using the 28 days UCS value of each sample as the final strength of

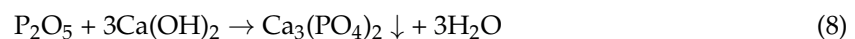
this study, the ratios of UCS growth values in 0–7 days, 7–14 days and 14–28 days to final strength are shown in Figure 11. It can be summarised that the UCS values of OCPB increased slowly at the early ages of hydration, ranging from 27.96% to 42.55%, and rapidly in the later stage, which strongly confirms the analysis of the soluble phosphate’s influence as noted above. By contrast, the values of TCPB all grew rapidly at the period of 0–7 days, ranging from 33.11% to 58.42%, and then gradually increased at the period of 7–28 days, which indicates that the strength formation of TCPB was mainly at 0–7 days. Therefore, water-washing pre-treatment can greatly reduce the retarding effect of PG on cement hydration in the early stage, however, with the hydration reaction, the mechanical property of PG-based CPB is still mainly determined by the mass concentration of mixture and the content of cement.



**Figure 11.** Growth rate ratio of UCS values of (a) OCPB, and (b) TCPB at different ages.

### 3.4. Microstructures of CPB

Figure 12 shows XRD patterns for the OCPB and TCPB (mix-proportion 3-OPG and 3-TPG) after 7, 14, and 28 days, the detected mineral phases are mainly  $\text{CaSO}_4 \cdot 2\text{H}_2\text{O}$ , Aft, and  $\text{SiO}_2$ . The probable reason that calcium silicate hydrate gel (C-S-H) cannot be detected in the XRD patterns is its amorphous or non-crystal micromorphology. As regards the  $\text{Ca}(\text{OH})_2$ , this can react with the impurities of PG, making the diffraction peak difficult to distinguish (compared with the main diffraction peaks). The reaction Equations are as follows [54]:



Based on the characteristic peaks of  $\text{CaSO}_4 \cdot 2\text{H}_2\text{O}$ , it can be concluded that the content of  $\text{CaSO}_4 \cdot 2\text{H}_2\text{O}$  both decreases gradually with the hydration of these two hydration systems. What’s more, compared with OCPB, the 7 days diffraction peaks of  $\text{CaSO}_4 \cdot 2\text{H}_2\text{O}$  in TCPB are not that strong in the XRD patterns illustrating that substantial  $\text{CaSO}_4 \cdot 2\text{H}_2\text{O}$  participates in the hydration system. However, as regards the 14, and 28 days diffraction peaks of  $\text{CaSO}_4 \cdot 2\text{H}_2\text{O}$ , TCPB are slightly stronger which may be associated with the inhibition effect of alkaline environment. A previous study [55] demonstrates that the hydration of  $\text{CaSO}_4 \cdot 0.5\text{H}_2\text{O}$  and  $\text{CaSO}_4 \cdot 2\text{H}_2\text{O}$  is inhibited by alkali, while a great quantity of acidic substances in TPG have been discharged with several water-washings that increased alkalinity of liquid phase in TCPB. Even so, the 7, 14, and 28 days diffraction peaks of Aft in TCPB were all greater than that of OCPB, which indicates that there were more hydration products and higher hydration degree in TCPB. Meanwhile, it can be observed that the 14, and 28 days characteristic peaks of Aft in OCPB increase significantly which further proves the disciplines of formation and destruction of the film, with the increase of curing time, the film in OCPB breaks and the hydration

reaction continues. That is to say, water-washing pre-treatment can effectively enhance the composition of hydration products of PG-based CPB and stimulate the formation of AFt in early ages.

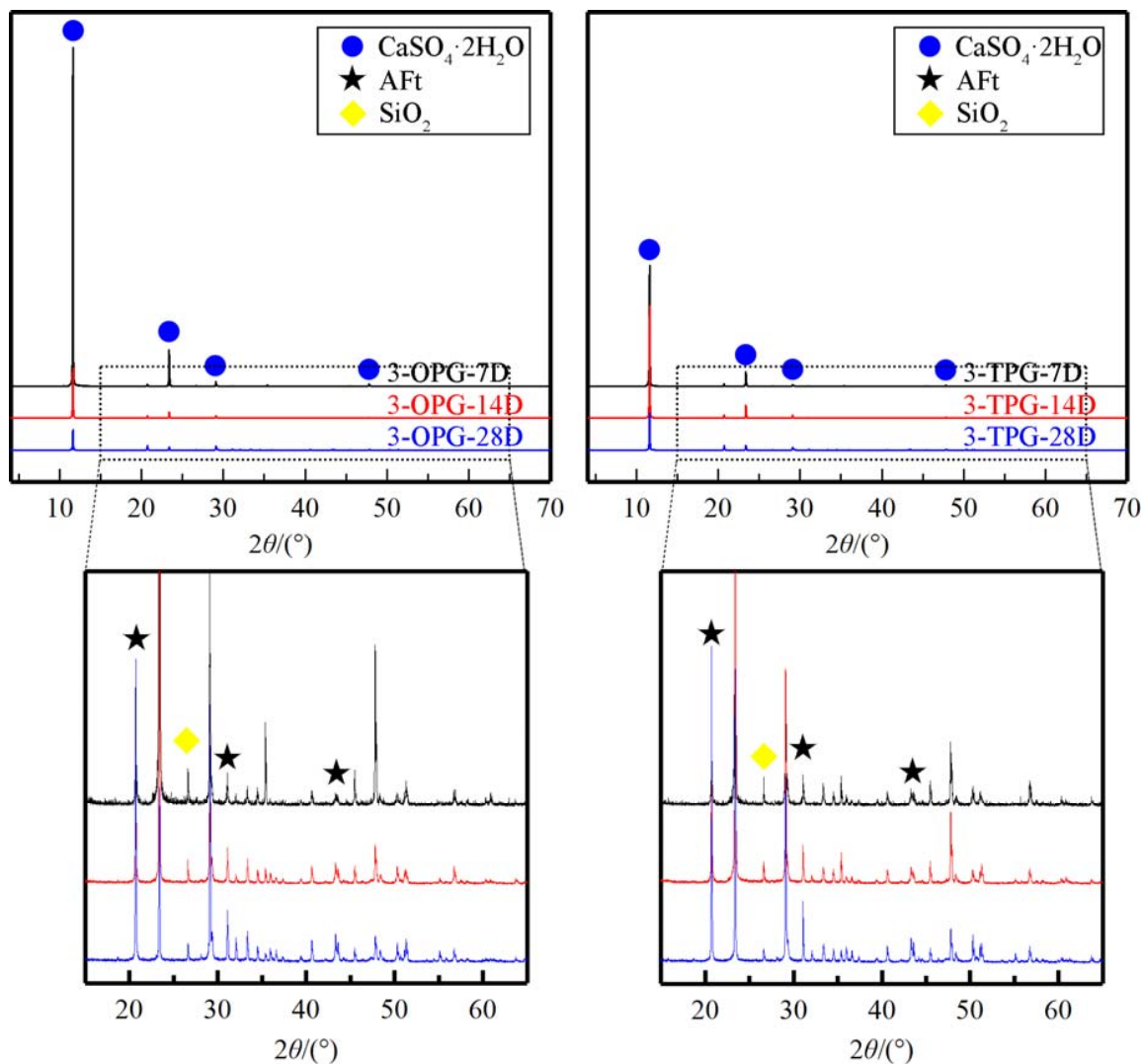
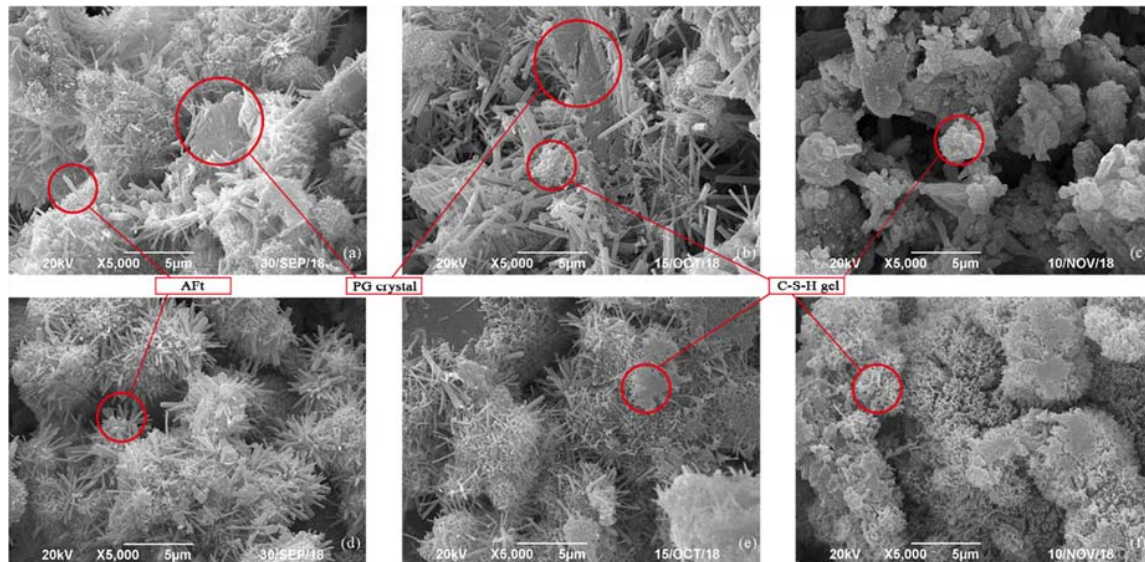


Figure 12. XRD patterns of OCPB and TCPB.

Subsequently, Figure 13 shows SEM images of the samples (Mix-proportion 3-OPG and 3-TPG) at different curing ages: left (Figure 13a,d) shows the morphology of specimens at 7 days, in the middle (Figure 13b,e) are specimens at 14 days, and on the right (Figure 13c,f) are at 28 days. These hydration products are needles, rods, or flocculants, among them, the needle or rod-like substances are ettringite (AFt). The floc material is CSH and covers the surfaces of the  $\text{CaSO}_4 \cdot 2\text{H}_2\text{O}$  crystal particles. By comparing Figure 13a–c with Figure 13d–f, it can be seen that the microstructure of hydration products of TCPB was better developed than OCPB at any curing time. As shown in Figure 13a, after 7 days of hydration, the prismatic and slab-like PG crystals in OCPB remained visible, even within image of 14 days. Besides, the impurities absorbed on PG crystal surface nearly gone and small amount of relatively tiny AFt was produced in the pores between the hydration products and  $\text{CaSO}_4 \cdot 2\text{H}_2\text{O}$  crystals. By contrast, from Figure 13d, although the pores of TCPB were not filled with hydration products, the microstructure was more compact with plenty of hydration products generating on the surface of PG particles. Figure 13c,f presents that a great deal of C-S-H gel both generated in OCPB and TCPB illustrating that the retarding effect of OPG decreased gradually with the hydration, while in OCPB, the generated C-S-H gel was much slenderer with huge pore size. Therefore, it can be

concluded that water-washing pre-treatment can effectively improve the microstructure of PG-based CPB by promoting the early hydration reaction and optimising the porosity of hydration system which improves the mechanical properties.



**Figure 13.** SEM images of OCPB samples with (a) 7 days, (b) 14 days, and (c) 28 days curing age and TCPB samples with (d) 7 days, (e) 14 days, and (f) 28 days curing age.

#### 4. Conclusions

This study investigated the feasibility of water-washing to pre-treat PG, aimed to improve the filling performance of PG-based CPB. Based on the considerable experimental results, the following conclusions were summarized as follows:

1. During the water-washing pretreatment, a certain number of soluble impurities on the surface of PG crystals could be removed by water-washing, and the morphology and size of the PG crystals were slightly optimized for CPB.
2. The water-washing pretreatment effectively improved the transport mobility and efficiency of the TCPB mixtures. The workability of the TCPB mixtures were greater than that of OCPB, which is beneficial to transport the TCPB to the stopes underground.
3. Moreover, because of the purification by water-washing, the impurities, which greatly hamper the hydration process, were separated from the OPG. The UCS value of TCPB was up to 2.45 times higher than that of OCPB samples. It can be concluded that the figures for TCPB increase significantly from stages of 0 to 7 days, and the purification capacity of water-washing by enhance the early UCS growth rate.
4. With the water-washing pretreatment, the diffraction peaks of AFt in the hydration system were also enhanced, although the diffraction peaks of some other hydration products were not found in the mineral phase due to the high PG content.

**Author Contributions:** Y.L., Q.Z. and Q.C. conceived the project; Y.L., Z.S. and Z.H. designed and performed the experiments; data curation, C.Q.; Y.L. wrote initial drafts of the work; Q.C. and Q.Z. wrote the final paper. All authors discussed the results and commented on the manuscript.

**Funding:** This essay is supported by the Fundamental Research Funds for the Central Universities of Central South University (2018zzts731) and Mittal Student Innovation Project of Central South University (201810533268).

**Conflicts of Interest:** The authors declare no conflict of interest.

## References

1. Howard, S.F.a.B.J. IAEA Technical Reports Series No. 475, Guidelines for Remediation Strategies to Reduce the Radiological Consequences of Environmental Contamination IAEA Safety Reports Series No. 78, Radiation Protection and Management of NORM Residues in the Phosphate Industry. *J. Radiol. Prot.* **2013**, *33*, 491–495. [[CrossRef](#)]
2. Bisone, S.; Gautier, M.; Chatain, V.; Blanc, D. Spatial distribution and leaching behavior of pollutants from phosphogypsum stocked in a gypstack: Geochemical characterization and modeling. *J. Environ. Manag.* **2017**, *193*, 567–575. [[CrossRef](#)] [[PubMed](#)]
3. Suárez, S.; Roca, X.; Gasso, S. Product-specific life cycle assessment of recycled gypsum as a replacement for natural gypsum in ordinary Portland cement: Application to the Spanish context. *J. Clean. Prod.* **2016**, *117*, 150–159. [[CrossRef](#)]
4. Yang, J.; Liu, W.; Zhang, L.; Xiao, B. Preparation of load-bearing building materials from autoclaved phosphogypsum. *Constr. Build. Mater.* **2009**, *23*, 687–693. [[CrossRef](#)]
5. Yang, L.; Yan, Y.; Hu, Z. Utilization of phosphogypsum for the preparation of non-autoclaved aerated concrete. *Constr. Build. Mater.* **2013**, *44*, 600–606. [[CrossRef](#)]
6. Liang, H.; Zhang, P.; Jin, Z.; DePaoli, D. Rare Earth and Phosphorus Leaching from a Flotation Aggregate of Florida Phosphate Rock. *Minerals* **2018**, *8*, 416. [[CrossRef](#)]
7. Chen, Q.; Zhang, Q.; Fourie, A.; Xin, C. Utilization of phosphogypsum and phosphate aggregate for cemented paste backfill. *J. Environ. Manag.* **2017**, *201*, 19–27. [[CrossRef](#)] [[PubMed](#)]
8. Abril, J.M.; Garcia-Tenorio, R.; Perianez, R.; Enamorado, S.M.; Andreu, L.; Delgado, A. Occupational dosimetric assessment (inhalation pathway) from the application of phosphogypsum in agriculture in South West Spain. *J. Environ. Radioactiv.* **2009**, *100*, 29–34. [[CrossRef](#)]
9. Yang, L.; Zhang, Y.; Yan, Y. Utilization of original phosphogypsum as raw material for the preparation of self-leveling mortar. *J. Clean. Prod.* **2016**, *127*, 204–213. [[CrossRef](#)]
10. Rajković, M.B.; Tošković, D.V. Phosphogypsum Surface Characterisation using Scanning Electron Microscopy. *Acta Periodica Technol.* **2003**, *34*, 61–70. [[CrossRef](#)]
11. Ali, M.A.; Lee, C.H.; Kim, S.Y.; Kim, P.J. Effect of industrial by-products containing electron acceptors on mitigating methane emission during rice cultivation. *Waste Manag.* **2009**, *29*, 2759–2764. [[CrossRef](#)]
12. Jiang, G.; Wu, A.; Wang, Y.; Lan, W. Low cost and high efficiency utilization of hemihydrate phosphogypsum: Used as binder to prepare filling material. *Constr. Build. Mater.* **2018**, *167*, 263–270. [[CrossRef](#)]
13. Chen, Q.; Zhang, Q.; Qi, C.; Fourie, A.; Xiao, C. Recycling phosphogypsum and construction demolition waste for cemented paste backfill and its environmental impact. *J. Clean. Prod.* **2018**, *186*, 418–429. [[CrossRef](#)]
14. Shen, W.; Gan, G.; Dong, R.; Chen, H.; Tan, Y.; Zhou, M. Utilization of solidified phosphogypsum as Portland cement retarder. *J. Mater. Cycles Waste* **2012**, *14*, 228–233. [[CrossRef](#)]
15. Yilmaz, E.; Belem, T.; Bussière, B.; Mbonimpa, M.; Benzaazoua, M. Curing time effect on consolidation behaviour of cemented paste backfill containing different cement types and contents. *Constr. Build. Mater.* **2015**, *75*, 99–111. [[CrossRef](#)]
16. Fall, M.; Benzaazoua, M.; Ouellet, S. Experimental characterization of the influence of aggregate fineness and density on the quality of cemented paste backfill. *Miner. Eng.* **2005**, *18*, 41–44. [[CrossRef](#)]
17. Cihangir, F.; Akyol, Y. Mechanical, hydrological and microstructural assessment of the durability of cemented paste backfill containing alkali-activated slag. *Int. J. Min. Reclam. Environ.* **2018**, *32*, 123–143. [[CrossRef](#)]
18. Ercikdi, B.; Cihangir, F.; Kesimal, A.; Deveci, H.; Alp, I. Utilization of water-reducing admixtures in cemented paste backfill of sulphide-rich mill Aggregate. *J. Hazard. Mater.* **2010**, *179*, 940–946. [[CrossRef](#)]
19. Cihangir, F.; Ercikdi, B.; Kesimal, A.; Ocak, S.; Akyol, Y. Effect of sodium-silicate activated slag at different silicate modulus on the strength and microstructural properties of full and coarse sulphidic aggregate paste backfill. *Constr. Build. Mater.* **2018**, *185*, 555–566. [[CrossRef](#)]
20. Dang, W.G.; Liu, Z.X.; He, X.Q.; Liu, Q.L.J.M.T. Mixture ratio of phosphogypsum in backfilling. *Min. Technol.* **2013**, *122*, 1–7. [[CrossRef](#)]
21. Shen, W.; Zhou, M.; Zhao, Q. Study on lime-fly ash-phosphogypsum binder. *Constr. Build. Mater.* **2007**, *21*, 1480–1485. [[CrossRef](#)]

22. Nizevičienė, D.; Vaičiukynienė, D.; Michalik, B.; Bonczyk, M.; Vaitkevičius, V.; Jusas, V.J.C.; Materials, B. The treatment of phosphogypsum with zeolite to use it in binding material. *Constr. Build. Mater.* **2018**, *180*, 134–142. [[CrossRef](#)]
23. Shen, Y.; Qian, J.; Huang, Y.; Yang, D. Synthesis of belite sulfoaluminate-ternesite cements with phosphogypsum. *Cem. Concr. Comp.* **2015**, *63*, 67–75. [[CrossRef](#)]
24. Li, X.; Du, J.; Gao, L.; He, S.; Gan, L.; Sun, C.; Shi, Y. Immobilization of phosphogypsum for cemented paste backfill and its environmental effect. *J. Clean. Prod.* **2017**, *156*, 137–146. [[CrossRef](#)]
25. Romero-Hermida, M.I.; Borrero-López, A.M.; Alejandre, F.J.; Flores-Alés, V.; Santos, A.; Franco, J.M.; Esquivias, L. Phosphogypsum waste lime as a promising substitute of commercial limes: A rheological approach. *Cem. Concr. Comp.* **2019**, *95*, 205–216. [[CrossRef](#)]
26. Taher, M.A. Influence of thermally treated phosphogypsum on the properties of Portland slag cement. *Resour. Conserv. Recycl.* **2007**, *52*, 28–38. [[CrossRef](#)]
27. Singh, M. Treating waste phosphogypsum for cement and plaster manufacture. *Cem. Concr. Res.* **2002**, *32*, 1033–1038. [[CrossRef](#)]
28. Mun, K.J.; Hyoung, W.K.; Lee, C.W.; So, S.Y.; Soh, Y.S. Basic properties of non-sintering cement using phosphogypsum and waste lime as activator. *Constr. Build. Mater.* **2007**, *21*, 1342–1350. [[CrossRef](#)]
29. Potgieter, J.H.; Potgieter, S.S.; McCrindle, R.I.; Strydom, C.A. An investigation into the effect of various chemical and physical treatments of a South African phosphogypsum to render it suitable as a set retarder for cement. *Cem. Concr. Res.* **2003**, *33*, 1223–1227. [[CrossRef](#)]
30. Kamimura, A.; Konno, E.; Yamamoto, S.; Watanabe, T.; Yamada, K.; Tomonaga, F. Improved method for the formation of recycled resins from depolymerized products of waste fiber-reinforced plastics: Simple and effective purification of recovered monomers by washing with water. *J. Mater. Cycles Waste* **2009**, *11*, 133–137. [[CrossRef](#)]
31. Slavinskaya, G.V. Water pretreatment to remove organic impurities and desalination with ion exchangers. *Russ. J. Appl. Chem.* **2003**, *76*, 1089–1093. [[CrossRef](#)]
32. Shuang, Y.; Hou, Y.; Zhang, B.; Yang, H.G. Impurity-Free Synthesis of Cube-Like Single-Crystal Anatase TiO<sub>2</sub> for High Performance Dye-Sensitized Solar Cell. *Ind. Eng. Chem. Res.* **2013**, *52*, 4098–4102. [[CrossRef](#)]
33. Ali, M.A.; Kim, P.J.; Inubushi, K. Mitigating yield-scaled greenhouse gas emissions through combined application of soil amendments: A comparative study between temperate and subtropical rice paddy soils. *Sci. Total Environ.* **2015**, *529*, 140–148. [[CrossRef](#)]
34. Cárdenas-Escudero, C.; Morales-Flórez, V.; Pérez-López, R.; Santos, A.; Esquivias, L. Procedure to use phosphogypsum industrial waste for mineral CO<sub>2</sub> sequestration. *J. Hazard. Mater.* **2011**, *196*, 431–435. [[CrossRef](#)]
35. *General Purpose Portland Cement*; B175-2007; Standardization Administration of China: Beijing, China, 2007.
36. *Environmental Quality Standards for Surface Water*; GB 3838-2002; Standardization Administration of China: Beijing, China, 2002.
37. *Integrated Wastewater Discharge Standard*; GB 8978-1996; Standardization Administration of China: Beijing, China, 1996.
38. *Mould for Concrete Specimens*; JG237-2008; Ministry of Housing and Urban-Rural Construction of the People's Republic of China: Beijing, China, 2008.
39. Wu, A.; Wang, Y.; Wang, H.; Yin, S.; Miao, X. Coupled effects of cement type and water quality on the properties of cemented paste backfill. *Int. J. Min. Process.* **2015**, *143*, 65–71. [[CrossRef](#)]
40. Liu, L.; Fang, Z.; Qi, C.; Zhang, B.; Guo, L.; Song, K.I.I.L. Numerical study on the pipe flow characteristics of the cemented paste backfill slurry considering hydration effects. *Powder Technol.* **2019**, *343*, 454–464. [[CrossRef](#)]
41. Qi, C.; Chen, Q.; Fourie, A.; Zhao, J.; Zhang, Q. Pressure drop in pipe flow of cemented paste backfill: Experimental and modeling study. *Powder Technol.* **2018**, *333*, 9–18. [[CrossRef](#)]
42. *Standard Test Method for Slump of Hydraulic-Cement Concrete*; C143/C143M-2015; American Society for Testing and Materials International (ASTM): West Conshohocken, PA, USA, 2015.
43. Qi, C.; Chen, Q.; Fourie, A.; Tang, X.; Zhang, Q.; Dong, X.; Feng, Y. Constitutive modelling of cemented paste backfill: A data-mining approach. *Constr. Build. Mater.* **2019**, *197*, 262–270. [[CrossRef](#)]
44. *Standard Test Methods for Compressive Strength of Cylindrical Concrete Specimens*; C39 C39M-2014a; American Society for Testing and Materials International (ASTM): West Conshohocken, PA, USA, 2015.

45. Liu, T. Study on Pretreatment and Application of Phosphogypsum. Master's Thesis, Wuhan University, Wuhan, China, 2010.
46. Wang, A.Q.; Zhang, C.Z.; Zhang, N.S. The theoretic analysis of the influence of the particle size distribution of cement system on the property of cement. *Cem. Concr. Res.* **1999**, *29*, 1721–1726. [[CrossRef](#)]
47. Sari, D.; Pasamehmetoglu, A.G. The effects of gradation and admixture on the pumice lightweight aggregate concrete. *Cem. Concr. Res.* **2005**, *35*, 936–942. [[CrossRef](#)]
48. Yao, W. Research and Application of High Concentration Filling Theory of Coarse Aggregate in Mines. Ph.D. Thesis, Kunming University of Science and Technology, Kunming, China, 2011.
49. Yang, J.-C.; Wu, H.-D.; Teng, N.-C.; Ji, D.-Y.; Lee, S.-Y. Novel attempts for the synthesis of calcium sulfate hydrates in calcium chloride solutions under atmospheric conditions. *Ceram. Int.* **2012**, *38*, 381–387. [[CrossRef](#)]
50. Ma, B.; Lu, W.; Su, Y.; Li, Y.; Gao, C.; He, X. Synthesis of  $\alpha$ -hemihydrate gypsum from cleaner phosphogypsum. *J. Clean. Prod.* **2018**, *195*, 396–405. [[CrossRef](#)]
51. Belem, T.; Benzaazoua, M. Design and application of underground mine paste backfill technology. *Geotech. Geol. Eng.* **2008**, *26*, 147–174. [[CrossRef](#)]
52. Li, M.; Moerman, A. Perspectives on the scientific and engineering principles underlying flow of mineral pastes. In Proceedings of the 34th Annual Meeting of CMP, Ottawa, ON, Canada, 22–24 January 2002; Paper No. 35. pp. 573–595.
53. Akin Altun, İ.; Sert, Y. Utilization of weathered phosphogypsum as set retarder in Portland cement. *Cem. Concr. Res.* **2004**, *34*, 677–680. [[CrossRef](#)]
54. Guo, C. Effect Mechanism of Fluorine and Phosphorus on Hydration Process of Cement Clinker. Ph.D. Thesis, Wuhan University of Technology, Wuhan, China, 2012.
55. Chen, X.; Gao, J.; Liu, C.; Zhao, Y. Effect of neutralization on the setting and hardening characters of hemihydrate phosphogypsum plaster. *Constr. Build. Mater.* **2018**, *190*, 53–64. [[CrossRef](#)]



© 2019 by the authors. Licensee MDPI, Basel, Switzerland. This article is an open access article distributed under the terms and conditions of the Creative Commons Attribution (CC BY) license (<http://creativecommons.org/licenses/by/4.0/>).